Noise Immunity-optimized Polarimeter Using Modified Polarization State Analyzer

Ping-Hsun Tsai, and Shang-Da Yang*
Institute of Photonics Technologies, National Tsing Hua University, Hsinchu 30013, Taiwan
Email:shangda@ee.nthu.edu.tw

Abstract: A new figure of merit (Poincaré angular error gradient) is proposed to optimize the noise immunity of polarimeter. The typical polarization state analyzer is modified to experimentally realize the optimized scheme.

I. INTRODUCTION

Measurement of the state of polarization (SOP) of electromagnetic waves is useful in remote sensing [1], astronomy [2], and high-speed fiber telecommunications where the bandwidth could be limited by polarization-mode dispersion (PMD) [3]. It is known that SOP can be determined by measuring the relative powers of (at least) four polarization components of the test SOP [4]. As a result, one or two rotatable retarders and one fixed polarizer (RRFP or 2RRFP) are used in analyzing the polarization components [5-7]. For example, 2RRFP-based polarization state analyzer (PSA) typically uses two quarter waveplates (QWPs) to transform the 0°-, 90°-, 45°-linearly polarized and the right-hand circularly polarized components of the test SOP into the *x*-polarization such that a linear polarizer can sample the corresponding powers [7]. PSA using single rotatable retarder still works, but can only sample a subset of polarization components [5]. As a result, it takes longer to calculate the SOP (matrix inversion is required) and the noise immunity optimization is subject to a tighter boundary condition. Optimization of the orientation angles and retardance of the single retarder in an RRFP polarimeter against random noise was carried out by minimizing the equally weighted variance (EWV) [5]. However, EWV is limited by some assumptions (equal noise for all measured powers, equal interest for all Stokes components), and the optimal 132° retarder is not an off-the-shelf optics. We proposed a geometrically intuitive figure of merit, Poincaré angular error gradient $\nabla\theta_\varepsilon$, to analyze the impact of random perturbation. A new set of four polarization components were searched by Monte Carlo algorithm to minimize the ensemble average of $|\nabla\theta_\varepsilon|$. To measure arbitrary polarization components, we replace one QWP in the 2RRFP by a half waveplate (HWP). Our experiments confirmed the feasibility of $\nabla\theta_\varepsilon$ and the improvement of the new 2RRFP configuration.

II. THEORY AND EXPERIMENT

Consider an incident light whose SOP can be represented by a Jones vector $\boldsymbol{J}\equiv[a_x,\ a_y\times e^{j\phi}]^T$, a Stokes vector $\boldsymbol{S}=[S_0,S_1,S_2,S_3]^T$, or $\boldsymbol{s}=[s_0,s_1,s_2,s_3]^T$, which are related by $S_0=(a_x)^2+(a_y)^2$, $s_0=(a_x)^2$, $S_1=(a_x)^2-(a_y)^2$, $s_1=(a_y)^2$, $S_2=s_2=2a_xa_y\cos\phi$, $S_3=s_3=2a_xa_y\sin\phi$. The power measurement vector, $\boldsymbol{p}=[p_1,\ p_2,\ p_3,\ p_4]^T$, is related to the test SOP via $\boldsymbol{p}=\boldsymbol{W}\times\boldsymbol{s}$, where $\boldsymbol{W}$ is a 4×4 matrix determined by the PSA. As a result, the vector $\boldsymbol{s}$ (thus SOP) can be calculated by $\boldsymbol{s}=\boldsymbol{W}^{-1}\times\boldsymbol{p}$ as long as $\boldsymbol{W}^{-1}$ exists. In the presence of perturbation, the four measured powers are modeled by $\boldsymbol{p}'=\boldsymbol{p}+\boldsymbol{\varepsilon}$ (the four elements of $\boldsymbol{\varepsilon}$, $\varepsilon_{1,2,3,4}$, are normalized to the total power S_0). The SOP measurement error can be described by the angle θ_ε between the measured Stokes vector $\boldsymbol{S}'=(S_1',S_2',S_3')$ and the actual one $\boldsymbol{S}=(S_1,S_2,S_3)$ (assuming S_0=1) [7]. The dependence of θ_ε on the perturbations $\varepsilon_{1,2,3,4}$ can be quantitatively characterized by a 4-D gradient vector

$$\nabla\theta_\varepsilon\equiv\left[\partial\theta_\varepsilon/\partial\varepsilon_1,\partial\theta_\varepsilon/\partial\varepsilon_2,\partial\theta_\varepsilon/\partial\varepsilon_3,\partial\theta_\varepsilon/\partial\varepsilon_4\right].$$

Since $\nabla\theta_\varepsilon$ depends on the test SOP, the chosen polarization components, or the bias error vector $\boldsymbol{\varepsilon}$, our goal is to find a set of four polarization components $\{\boldsymbol{J}_{1,2,3,4}\}$ corresponding to the lowest ensemble average E of $|\nabla\theta_\varepsilon(\boldsymbol{\varepsilon}=\boldsymbol{0})|$, where $E\equiv\sum_{n=1}^{N}\left|\nabla\theta_\varepsilon\right|_n\times w_n$, w_n is the relative solid angle of the nth possible SOP on the Poincaré sphere.

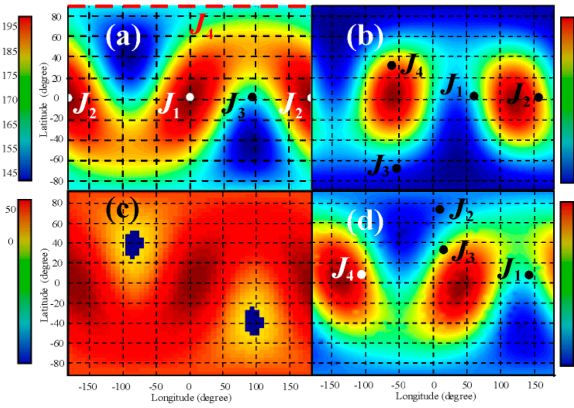

Fig.1. Distributions of Poincaré angular error gradient magnitude of (a) standard 2RRFP, (b) optimized 2RRFP, (c) difference between (a) and (b), and (d) EWV-optimized RRFP obtained in [5], respectively.

Figure 1(a) shows the distribution of gradient magnitude $|\nabla\theta_\varepsilon|$ due to the standard 2RRFP-based PSA using $\{\boldsymbol{J_1}=[1,0]^T,\ \boldsymbol{J_2}=[0,1]^T,\ \boldsymbol{J_3}=2^{-0.5}\times[1,1]^T,\boldsymbol{J_4}=2^{-0.5}\times[1,j]^T\}$, corresponding to an ensemble average of E_0=182.070°. This means a signal-to-noise ratio (SNR) of 10^2 ($\varepsilon_i\sim10^{-2}$) may incur a Poincaré angular error of $\theta_\varepsilon\sim$1.82°. By using

Monte Carlo algorithm, we got a new set of four polarization components

$$\boldsymbol{J}_1=\begin{bmatrix}0.89\\0.45\angle 7.5^\circ\end{bmatrix},\boldsymbol{J}_2=\begin{bmatrix}0.20\\0.98\angle 10.7^\circ\end{bmatrix},\boldsymbol{J}_3=\begin{bmatrix}0.79\\0.62\angle -107.7^\circ\end{bmatrix},\boldsymbol{J}_4=\begin{bmatrix}0.81\\0.59\angle 146.9^\circ\end{bmatrix},$$

leading to a reduced ensemble average E=142.894° (EWV=10.3). The corresponding gradient magnitude distribution [Fig. 1(b)] is lower than that of the standard 2RRFP except for a nominal fraction (~2%) of all possible SOPs [Fig. 1(c), blue area]. Surprisingly, the four EWV-optimized polarization components proposed in [5] correspond to a slightly lower ensemble average E=140.454° (EWV=10.0) under our definition [Fig. 1(d)]. No better result can be found by using the EWV-optimized solution as the initial condition to our Mote Carlo codes. This implies a complicated potential surface of E that is prone to trapping the optimization process by local minima.

The experimental setup is shown in Fig. 2. The light source is a distributed feedback laser operated at 1550 nm. The linear polarizer (LP) and the first QWP (QWP1) are utilized to generate test SOPs, while the remaining components are responsible of SOP measurement. A half waveplate (HWP) replaces the second QWP in a standard 2RRFP PSA such that the four "optimized" polarization components $\{\boldsymbol{J}_{1,2,3,4}\}$ can be measured by proper orientation angles θ_1, θ_2 of QWP2 and HWP (Table 1).

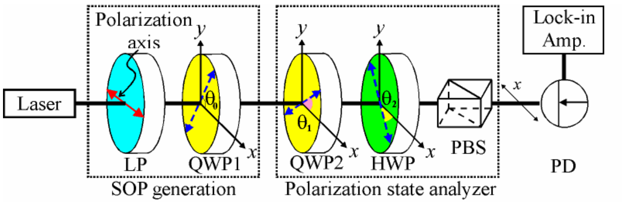

Fig. 2. Experimental setup. LP: Linear polarizer. Q(H)WP: λ/4(λ/2) waveplate. PBS: Polarization beam splitter. PD: Photodetector.

Table 1. The orientation angles of QWP1 and HWP to measure the four optimized polarization components.

	$\boldsymbol{J}_1$	$\boldsymbol{J}_2$	$\boldsymbol{J}_3$	$\boldsymbol{J}_4$
θ_1 (QWP)	26.9°	-11.5°	-25.4°	-34.2°
θ_2 (HWP)	15.0°	38.2°	150.4°	170.7°

We experimentally suppressed the impact of deterministic perturbations by using the calibration procedure [4,7], such that $\boldsymbol{\varepsilon}$ can be modeled by a vector of zero-mean random variables. The Poincaré angular error predicted by an inner product $\theta_\varepsilon=(\nabla\theta_\varepsilon)\cdot\boldsymbol{\varepsilon}$, however, is not zero-mean (for $\theta_\varepsilon>0$). For simplicity, we estimate the mean of Poincaré angular error by using a constant vector $\kappa\times\boldsymbol{\sigma}$ in place of $\boldsymbol{\varepsilon}$, where κ is a constant to be determined and $\sigma_{1,2,3,4}$ are the (normalized) standard deviations of the four measured powers $p'_{1,2,3,4}$. In Fig. 3(a), 48 data points corresponding to 9 different SOPs [including 0°-, 45°-, 90°-linear polarizations, right-hand circular (RHC) polarization, and 5 different elliptical polarizations] and different noise powers $|\boldsymbol{\sigma}|$ (ranging from 4×10^{-4} to 4.5×10^{-2} of the total power) are presented. The correlation coefficient between the predicted and experimentally measured angular errors, i.e. $\theta_\varepsilon/\kappa$ and θ'_ε, is 0.935. The fit line in Fig. 3(a) indicates a quasi-linear relation θ'_ε =0.353 × $(\theta_\varepsilon/\kappa)^{0.957}$, suggesting a scaling constant of κ=0.353. Fig. 3(b) shows that the optimized 2RRFP configuration gives lower angular error compare with the standard 2RRFP counterpart when measuring 9 different SOPs under different noise powers (20 data points).

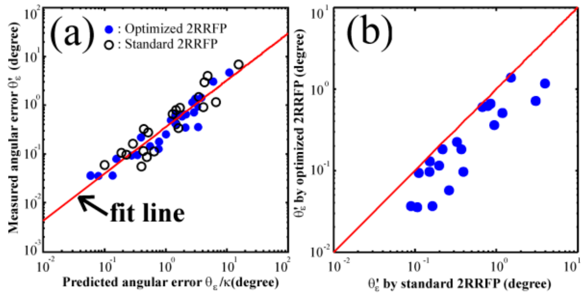

Fig. 3. Relation between the Poincaré angular errors obtained by (a) prediction and experiment, (b) experiments using optimized and standard 2RRFP configurations, respectively.

III. CONCLUSIONS

A new figure of merit, Poincaré angular error gradient, is proposed to optimize the noise immunity of polarimeter. The standard 2RRFP polarization state analyzer is modified by replacing one QWP by a HWP to realize the optimized scheme. Experiments confirmed that Poincaré angular error gradient can quantitatively predict the SOP measurement error, and the optimized scheme does outperform the standard one.

ACKNOWLEDGMENT

This material is based on research supported by the National Science Council in Taiwan under grants NSC 100-2221-E-007-093-MY3, 99-2120-M-007-010 and by the National Tsing Hua University under grant 100N2081E1.

REFERENCES

[1] A. Sadjadi and S. L. Chun, "Remote sensing using passive infrared Stokes polarimeter", *Opt. Eng.*, **43**(10), 2283-2291 (2004).

[2] A. M. Gandorfer, "Ferroelectric retarders as an alternative to piezoelastic modulators for use in solar Stokes vector polarimetry", *Opt. Eng.*, **38**(8), 1402-1408 (1999).

[3] D. L. Peterson Jr., B. C. Ward, K. B. Rochford, P. J. Leo, and G. Simer, "Polarization mode dispersion compensator field trial and field fiber characterization", *Opt. Express*, **10**(14), 614-621 (2002).

[4] R. A. Chipman, and M. Bass, *Handbook of Optics, Volume 2, 2nd edition*. McGraw-Hill, New York, 1995.

[5] D. S. Sabatke, M. R. Descour and E. L. Dereniak, "Optimization of retardance for a complete Stokes polarimeter", *Opt. Lett.*, **25**(11), 802-804 (2000).

[6] L. Gendre, A. Foulonneau, and L. Bigué, "Full Stokes polarimetric imaging using a single ferroelectric liquid crystal device", *Opt. Eng.*, **50**(8), 081209-1-9 (2011).

[7] S. X. Wang and A. M. Weiner, "Fast wavelength-parallel polarimeter for broadband optical networks", *Opt. Lett.*, **29**(9), 923-925 (2004).